Compact oleic acid in HAMLET.

Fast, Jonas; Mossberg, Anki; Nilsson, Hanna; Svanborg, Catharina; Akke, Mikael; Linse, Sara

Published in:
FEBS Letters

DOI:
10.1016/j.febslet.2005.08.089

2005

Compact oleic acid in HAMLET

Jonas Fast[‡||*], Ann-Kristin Mossberg[†], Hanna Nilsson[‡], Catharina Svanborg[†], Mikael Akke[‡], and Sara Linse[‡*]

[‡]Department of Biophysical Chemistry, Lund University,

[†]Department of Microbiology, Immunology and Glycobiology, Lund University

[||]Present address: Department of Chemistry and Biochemistry, University of Colorado, Cristol Building, room 226, Boulder, CO 80309-0215, USA.

*corresponding authors: sara.linse@bpc.lu.se, tel/fax: + 46 46 222 82 46/45 43, P O Box 124, SE-221 00 Lund, Sweden. jfast@colorado.edu, tel: + 1 303 492 2369,

Abstract

HAMLET (human alpha-lactalbumin made lethal to tumor cells) is a complex between α-lactalbumin and oleic acid that induces apoptosis in tumor cells, but not in healthy cells. Heteronuclear NMR spectroscopy was used to determine the structure of ^{13}C- oleic acid in HAMLET, and to study the ^{15}N-labeled protein. Nuclear Overhauser enhancement spectroscopy shows that the two ends of the fatty acid are in close proximity and close to the double bond, indicating that the oleic acid is bound to HAMLET in a compact conformation. The data further show that HAMLET is a partly unfolded/molten globule-like complex under physiological conditions.

Keywords: Nuclear magnetic resonance, HAMLET, oleic acid, α-lactalbumin[1]

[1] Abbreviations: CD, circular dichroism, EDTA; ethylenediamintetraacetic acid, HAMLET; human alpha-lactalbumin made lethal to tumor cells, HSQC; heteronuclear single quantum correlation, MD; molecular dynamics, NMR; nuclear magnetic resonance, NOESY; nuclear Overhauser enhancement spectroscopy.

1. Introduction

HAMLET is a complex of human α-lactalbumin and oleic acid (Fig 1a), which induces apoptosis in tumor cells, but spares healthy cells [1]. The anti-tumor activity includes over 40 different lymphoma and carcinoma cell lines [2]. HAMLET removes skin papilloma in patients [3] and limits the progression of human glioblastoma in a rat xenograft model [4]. HAMLET binds to the surface of tumor cells, enters the cells, interacts with mitochondria [5], targets ribosomes and activates caspases [6]. Eventually the protein accumulates in the cell nucleus where it interacts with histones and disrupts chromatin structure [7].

HAMLET is produced from α-lactalbumin through removal of bound Ca^{2+} and exposure to oleic acid on an ion exchange column [8,9]. HAMLET is eluted as a complex of fatty and protein and has the characteristics of a protein that is kinetically trapped in a partly folded state [10]. It has not been possible to produce the active complex by mixing the pure components in solution [1].

Here we use heteronuclear NMR spectroscopy to characterize the structure of the protein and the fatty acid in HAMLET. The results show that oleic acid is bound to HAMLET in a compact fashion and that HAMLET is a partly unfolded molten globule-like complex at physiological conditions.

2. Materials and methods

Expression and purification of α–lactalbumin

Native α-lactalbumin was purified from human milk as described [1]. ^{15}N-labeled recombinant human α-lactalbumin was expressed from the pAla plasmid (kindly provided by Peter S Kim [29]) in *Eschericia coli* BL21 DE3 cells in M9 minimal medium containing 98% enriched $^{15}NH_4Cl_2$ using standard procedures. The cell pellet was sonicated in 20 mM Tris/HCl, pH 7.5, and inclusion bodies were collected by centrifugation, resonicated, and dissolved by shaking overnight in 20 mM Tris/HCl, pH 8.0, 8 M urea,10 mM reduced glutathione. The solution was applied to a DEAE cellulose column at room temperature, washed with 20 mM Tris/HCl (pH 8.0), 10 mM reduced glutathione. 0.25 M KCl, and eluted with 20 mM Tris/HCl (pH 8.0), 0.5 M KCl, 10 mM reduced glutathione, 7 M urea. The eluate was dialysed against standing tap water (twice the eluate volume) for 24 hours, and against slowly running tap water for 48 hours. A water hose with an open side hole was used to facilitate air oxidation. The folded protein was purified using ion exchange chromatography on a DEAE Sephacel column in 20 mM Tris/HCl, pH 7.8, 1 mM $CaCl_2$, and eluted using a linear salt gradient up to 0.2 M NaCl in the same buffer. The purity of the protein was confirmed by agarose gel electrophoresis, SDS-PAGE, and ^{1}H-NMR spectroscopy.

HAMLET production

^{15}N-labeled human recombinant α-lactalbumin or human milk α-lactalbumin, was converted to HAMLET with fully ^{13}C-labeled oleic acid (Martek Bioscience Corp.,

Columbia, MD, USA) using the method described before [1]. The activity of lyophilized HAMLET against tumor cells was confirmed as described [1].

NMR samples

Lyophilized HAMLET (5-15 mg) was dissolved in 350-500 µl H_2O containing 5–10% D_2O, 0.15 M NaCl, 0.1 mM NaN_3, and 1 mM DSS at pH 7.3-7.5. The samples were transfered into 5 mm Shigemi tubes and sealed.

NMR Spectroscopy

2D proton and heteronuclear NMR spectra were recorded on a Varian Unity Inova 500 MHz NMR spectrometer using 5 mm inverse or triple resonance probes with pulsed field gradient capabilities. The ^{1}H carrier was set to the water frequency, the ^{15}N carrier to 119 ppm, and the ^{13}C carrier to 45 ppm for methyl and methylene carbons, or 130 ppm for methine carbons. Water presaturation was used. ^{1}H-^{15}N HSQC spectra were recorded with spectral widths of 6000 Hz for ^{1}H and 1800 Hz for ^{15}N, using 2048 and 128 complex data points in the acquisition (t_2), and indirect (t_1) dimensions, respectively. ^{1}H-^{13}C HSQC spectra were recorded with spectral widths of 10,000 Hz for ^{1}H and 6000 Hz for ^{13}C using 2048 and 256 complex data points in the t_2 and t_1 dimension, respectively. 3D ^{13}C-edited ^{1}H-^{1}H NOESY-HSQC spectra were recorded for unlabeled protein and ^{13}C-labeled oleic acid at 20 and 37 °C with spectral widths of 6000 and 5600 Hz in the ^{1}H dimension (t_1 and t_2) and 10,000 Hz in the ^{13}C dimension (t_3) using 4096, 2048 and 512 complex data points, respectively. The mixing time was 50 ms. ^{13}C-edited COSY and ^{13}C-edited TOCSY spectra for oleic acid peak assignments were acquired using spectral

widths of 8000 Hz for ^{1}H using 4288 and 300 complex points, respectively, in the two ^{1}H dimensions. Spectra were processed using a fourth order polynomial solvent filter, Lorentzian/Gaussian and sine-bell window functions in the direct and indirect dimensions, respectively, and zero filling to twice the number of collected data points. NMRPipe, NMRDraw [11] and Sparky (T.D. Goddard & D.G. Kneller (2003), University of California, San Fransisco) were used for processing and analysis of NMR data.

Structure calculations of bound and free oleic acid

Distance restraints were derived from the cross-peak volumes in NOESY spectra (Table 2), as calculated by fitting a Gaussian line-shape to each cross-peak using the program Sparky. The cross-peak between C2H and C3H was used for calibration, assuming an average proton-proton distance of 2.3 Å. In case of overlap, the volumes were divided by the product of the numbers of possible contributing protons in each group, thus yielding an upper limit on the distance. The Gromacs molecular dynamics (MD) software package [12,13] was used to calculate a model of oleic acid in HAMLET. A topology file for oleic acid was constructed on the PRODRG server [14], using the oleic acid structure in liver fatty acid binding protein (L-FABP, PDB accession number 1LFO) as a template. The simulations used the Gromacs force field, *ffgmx2*, which is based on the GROMOS-87 force field [15], and a simple point charge (SPC) model for water molecules. One oleate molecule was put in a cubic box with one sodium counter ion and 284 water molecules. The starting structure was subjected to energy minimization using a steepest descent algorithm, followed by a 5 nanoseconds (2500 000 time steps) long MD simulation at

310 K and 1 bar using Berendsen temperature and pressure coupling [16]. The radius of gyration was used to monitor when equilibrium was established. Two MD simulations were performed, one without ("non-restrained") and one with ("restrained") NMR-derived distance restraints included with high standard force constants. An ensemble of 10 MD structures was collected at 500 ps intervals from 500 to 5000 ps. The structures were aligned and visualized using the Molmol software [17].

3. Results and discussion

NMR spectra of unbound and bound oleic acid

The ^{1}H and ^{13}C assignments for free and bound oleic acid were performed using ^{13}C-edited COSY spectra to work out the scalar couplings along the carbon chain, and are reported in Table 1 and Figure 1. Chemical shift differences are observed between the two states, implying that the local magnetic field changes upon binding to the protein. The ^{13}C-edited ^{1}H-^{1}H NOESY-HSQC spectra of uniformly ^{13}C-labelled oleic acid in water contain only a small set of NOE cross-peaks between protons that are close in sequence (Figure 1c); hence, the fatty acid is predominantly extended, and/or interconverts between a large number of energetically equivalent conformations.

The ^{13}C-edited ^{1}H-^{1}H NOESY-HSQC spectra of oleic acid in HAMLET are similar at 37 °C (Figure 1b,d) and 20 °C (data not shown). These spectra have broader lines compared to free fatty acid, reflecting a slower rotational diffusion of the protein-oleic acid complex. This verifies that oleic acid is bound with high affinity in the complex. Strong NOE cross peaks are observed between the ends of the fatty acid chain (Figure 1). This

implies that the fatty acid is folded so that these protons at the two ends are close to one another. Alternatively, two molecules of oleic acid interacting in an anti-parallel fashion would also yield cross-peaks between the two ends. However, stoichiometry studies of the complex have indicated that one oleic acid is bound per α-lactalbumin chain [8], making this interpretation less likely. While a 2:2 complex would be consistent with both the NOE's and the stoichiometry, gel filtration indicates that dimers or higher order oligomers represent a maximum of 2-5 % of the sample (data not shown). Furthermore, magnetic resonance dispersion (MRD) measurements [30] show that there is a maximum of 5% dimers in a 1.3 mM HAMLET sample with no added calcium or salt (M. Gottschalk, personal communication). Based on this result, together with the fact that the NOE between the two ends of oleic acid is of comparable intensity with those of the NOEs between vicinal protons (Table 2), we conclude that the end-to-end NOE cannot be dominated by the small population of dimer, but must be present also in the monomeric population. The NOEs between each end and the protons surrounding the double bond suggest a further coiling of the fatty acid to yield a significantly compacted structure.

Fatty acid structure

MD simulations based on the present data were used to provide a structural view of oleic acid in HAMLET compared to free oleic acid. The restraints listed in Table 2 include two unambiguous NOEs, CH2-CH18 and CH3-CH18, in addition to a strong cross peaks between CH18 and CH8/11, two medium cross peaks between CH2 and CH8/11 and between CH3 and CH8/11, and a weak cross-peak between CH18 and CH9/10. These six constraints were used as distance restraints in one MD simulation. A parallel simulation

was performed without restraints. The radius of gyration reached a stable value after 350 ps in both the restrained and non-restrained simulation. The 10-membered ensemble from the restrained simulation has an RMSD of 2.0 Å. As seen in Figure 2a, there are a number of similar conformations that fulfil all the NOE constraints, and all of them are significantly compacted. The ensemble hence reveals a compact structure in which the two ends are close to one another and also close to the *cis* double bond. The binding of oleic acid in a preferred conformation suggests specificity in its interactions with the protein. A compact oleic acid can be accommodated in a hydrophobic cleft as suggested [8], while a straight fatty acid would reach through/across the protein. A number of protein structures with bound oleic acid have been reported, with both extended and U-shaped fatty acid (Figure 2c).

Without restraints, the MD simulation yields an extended oleic acid conformation (Figure 2b) with an RMSD of 2.6 Å. The larger RMSD compared to the restrained simulation reflects a larger conformational freedom of the free oleic acid.

Fatty acid-protein contacts

Close proximity between specific protein moieties and bound oleic acid gives rise to NOE cross peaks. Positive NOE cross-peaks are observed between oleic acid protons resonating at 1.3 ppm (i.e. protons on carbons 4–7 and/or 12–15) and protein resonances at 4 and 7 ppm (marked ** in Fig. 1d) with temperature-dependent intensities. These cross peaks are severely broadened due to conformational exchange dynamics, and could not be assigned to specific amino acids nor aid in locating the fatty acid binding site,

since statistically, the protein chemical shifts of the NOESY cross peaks can occur for virtually all amino acid types (http://www.bmrb.wisc.edu/). In addition, negative NOE cross-peaks are observed between oleic acid and water, which could implicate long-lived water molecules in the vicinity of the bound oleic acid [18]. Alternatively, these cross peaks may be mediated by exchange between water and labile protons in the protein side chains that are close to the bound oleic acid [19].

Protein chain

Random coil and largely unstructured protein segments give narrow NMR signals and limited dispersion of proton resonances, but better dispersion of nitrogen resonances. Folded proteins yield broader signals, and large chemical shift dispersion, and this is seen also for native human α-lactalbumin (C. Redfield, personal communication). Molten globules and partly folded proteins yield very poor dispersion and severe line broadening. $^{1}H^{-15}N$ HSQC spectra of HAMLET at 15, 20, 27, and 37 °C (Fig. 3) have poor chemical shift dispersion and a limited number of signals. The spectrum at 37 °C has only a small number of resolved peaks and several broad signals. The NMR spectra for HAMLET are distinctly different from those of native and apo α-lactalbumin, with fewer resolved peaks, yet contain a larger number of signals than the pH 2 molten globule of human or bovine α-lactalbumin that yield only a few N-terminal peaks [25-28]. Instead, the ^{1}H-^{15}N HSQC spectra of HAMLET are similar to the pH 2 spectrum for guinea pig α-lactalbumin [25] with a somewhat larger number of resonances. Resonances from side chain amides appear at 7.5/113 and 6.8/113 ppm, while most other signals from HAMLET are clustered between 7.5 and 8.7 ppm in the ^{1}H dimension. (The signal that

moves from 5.8/109.5 to 5.8/113.5 ppm at 37°C is a folded Arg side chain resonance.) At 37°C, two peaks are found at 10.4 and 10.2/131 ppm that are attributed to tryptophan indole N-H. The resolution is marginally better at lower temperature, but the overall features remain the same. Clearly, there are two sets of signals, one set of relatively narrow lines and one set of severely broadened resonances. The number of narrow signals increases with decreasing temperature, presumably due to a decrease of the rate of amide proton exchange with solvent in the unfolded regions that give rise to these narrow peaks. The largest changes in the spectra occur between 27 and 37°C, and around 20% of the resonances in the protein are visible at 15 °C. This is the same temperature range where the largest changes are observed in the near-UV CD spectrum of HAMLET [10]. Together, these results imply changes in tertiary interactions, corresponding to either a shift in the average coordinate positions or to a narrowing of the coordinate distributions In contrast, the far-UV CD spectrum is largely unaffected across this temperature range, implying that secondary structure is largely maintained [10]. The NMR spectral characteristics of HAMLET suggest a partially folded structure in fast to intermediate exchange. There is no indication of extensive aggregation under the present conditions (cf. above).

The classical molten-globule like states of α-lactalbumin are not significantly populated under physiological conditions, but are induced by changes in environmental parameters, for example by lowering the pH, raising the temperature, or adding EDTA, reducing agent or denaturant [20-23]. In contrast, the kinetically trapped HAMLET retains its molten globule-like characteristics at physiological conditions [1,9,10,24]. This property,

as well as the anti -tumor activity of HAMLET, are strictly dependent on the presence of bound oleic acid or vaccenic acid [8]. While both straight and compact conformations of oleic acid are observed in the structures of other fatty acid binding proteins (with examples in Figure 2c), α-lactalbumin apparently needs to bind the fatty acid in a compact conformation in order to convert into HAMLET, yielding an altered structure with a new function. In conclusion, HAMLET is both structurally and functionally distinct from other known oleic acid binding proteins.

4. Acknowledgements

We thank FAA Mulder and P Lundström for NMR assistance, and I André for help with the MD simulations. We thank M. Gottschalk for help with NMR dispersion measurements. This study was supported by the Swedish Research Council.

5. References

[1] Svensson, M., Hakansson, A., Mossberg, A.K., Linse, S. and Svanborg, C. (2000) Proc Natl Acad Sci U S A 97, 4221-6.
[2] Håkansson, A. (1999) Lund University, Lund.
[3] Gustafsson, L., Leijonhufvud, I., Aronsson, A., Mossberg, A.-K. and Svanborg, C. (2004) N Engl J Med 350, 2663-2672.
[4] Fischer, W., Gustafsson, L., Mossberg, A.-K., Gronli, J., Mork, S., Bjerkvig, R. and Svanborg, C. (2004) Cancer Res 64, 2105-2112.
[5] Kohler, C., Gogvadze, V., Hakansson, A., Svanborg, C., Orrenius, S. and Zhivotovsky, B. (2001) Eur J Biochem 268, 186-91.
[6] Svanborg, C. et al. (2003) Adv Cancer Res 88, 1-29.
[7] Duringer, C., Hamiche, A., Gustafsson, L., Kimura, H. and Svanborg, C. (2003) J Biol Chem.
[8] Svensson, M., Mossberg, A.-K., Pettersson, J., Linse, S. and Svanborg, C. (2003) Protein Sci 12, 2805-2814.
[9] Svensson, M., Sabharwal, H., Hakansson, A., Mossberg, A.K., Lipniunas, P., Leffler, H., Svanborg, C. and Linse, S. (1999) J Biol Chem 274, 6388-96.
[10] Fast, J., Mossberg, A.-K., Svanborg, C. and Linse, S. (2005) Protein Science.
[11] Delaglio, F., Grzesiek, S., Vuister, G.W., Zhu, G., Pfeifer, J. and Bax, A. (1995) J Biomol NMR 6, 277-93.
[12] Lindahl, E., Hess, B. and van der Spoel, D. (2001) Journal of Molecular Modeling 7, 306-317.
[13] Berendsen, H.J.C., Vanderspoel, D. and Vandrunen, R. (1995) Computer Physics Communications 91, 43-56.
[14] vanAalten, D.M.F., Bywater, R., Findlay, J.B.C., Hendlich, M., Hooft, R.W.W. and Vriend, G. (1996) Journal of Computer-Aided Molecular Design 10, 255-262.
[15] van Gunsteren, W.F. and Berendsen, H.J.C. (1987), Biomos BV Nijenborgh 4, 9747 AG Groningen, The Netherlands.
[16] Berendsen, H.J.C., Postma, J.P.M., Vangunsteren, W.F., Dinola, A. and Haak, J.R. (1984) Journal of Chemical Physics 81, 3684-3690.
[17] Koradi, R., Billeter, M. and Wuthrich, K. (1996) J Mol Graph 14, 51-56.
[18] Otting, G. (1997) Progress in Nuclear Magnetic Resonance Spectroscopy 31, 259-285.
[19] Denisov, V.P. and Halle, B. (1996) Faraday Discuss, 227-44.
[20] Dolgikh, D.A. et al. (1985) Eur Biophys J 13, 109-21.
[21] Pfeil, W., Bychkova, V.E. and Ptitsyn, O.B. (1986) FEBS Lett 198, 287-91.
[22] Veprintsev, D.B., Permyakov, S.E., Permyakov, E.A., Rogov, V.V., Cawthern, K.M. and Berliner, L.J. (1997) FEBS Lett 412, 625-8.
[23] Kuwajima, K. (1996) Faseb J 10, 102-9.
[24] Svensson, M. et al. (2003) Protein Sci 12, 2794-2804.
[25] Kim, S. and Baum, J. (1998) Protein Sci 7, 1930-8.
[26] Wijesinha-Bettoni, R., Dobson, C.M. and Redfield, C. (2001) J Mol Biol 307, 885-98.
[27] Schulman, B.A., Kim, P.S., Dobson, C.M. and Redfield, C. (1997) Nat Struct Biol 4, 630-4.

[28] Ramboarina, S. and Redfield, C. (2003) Journal of Molecular Biology 330, 1177-1188.

[29] Peng, Z., Wu, L.C. and Kim, P.S. (1995) Biochemistry 34, 3248-3252.

[30] Halle, B., and Denisov, V. P. (2001). Magnetic relaxation dispersion studies of biomolecular solutions. Methods Enzymol *338*, 178-201.

6. Figure legends

Figure 1. 2D projection from 3D ^{13}C-edited ^{1}H-^{1}H NOESY-HSQC spectra of oleic acid in the HAMLET-bound (b, d) and free (c) states at 37 ^{o}C. Resonances are labelled according to the numbering scheme shown in (a). Resonances from residual EDTA (*), and cross-peaks between oleic acid and protein (**) or water (***) are indicated.

Figure 2. Snap shots from the restrained simulation of oleic acid in HAMLET (a), and the mean structure from the unrestrained (b) simulation of oleic acid in water. Examples of oleic acid bound to liver fatty acid binding protein (1lfo) and human serum albumin (1gni) are given in (c). The carboxylic oxygens are shown in black, the double bond carbons in dark grey and the rest of the carbon chain in grey. The Figure was produced using MolMol software [17].

Figure 3. ^{15}N HSQC spectra of HAMLET in 0.15 M NaCl, pH 7.4 at (a) 15°C; (b) 20°C; (c) 27°C; (d) 37°C. All spectra were plotted using a signal threshold set just above the noise level in spectrum (d).

7. Tables and Figures

Table 1. ^{1}H and ^{13}C chemical shifts (δ, ppm) for free and bound oleic acid.

Carbon n:o*	**δ (^{1}H, free)**	**δ (^{1}H, bound)**	**δ (^{13}C, free)**	**δ (^{13}C, bound)**
2	2.29	2.24	38.01	39.72
3	1.64	1.60	28.06	28.84
8/11	2.09	2.02	30.08	29.62
9/10	5.43	5.33	132.38	132.88/131.97
18	0.96	0.90	16.87	16.72
4-7, 12-15	1.39	1.30	32.41	32.40
17	1.44[#]	1.43	25.89[#]	23.09
16	1.35	1.29	34.90	34.74
X	1.37	1.32	25.28	25.42

* Protons are numbered according to their attached carbon, see Figure 1a. [#]overlapped

X not assigned.

Table 2. NOE crosspeak volumes. The scaling factor based on the product of the number of protons potentially contributing to the cross peaks and the calculated NOE distances are provided for the constraints used in the restrained MD simulation.

Cross peaks	**NOE Volume**	**scaling factor**	**Distance (Å)**
2⇔3	$2.0 \cdot 10^9$	4	2.30[#]
2⇔8/11	$8.0 \cdot 10^8$	8	3.01
2⇔*	$6.4 \cdot 10^9$		
2⇔18	$2.1 \cdot 10^9$	6	2.44
3⇔8/11	$6.7 \cdot 10^8$	8	3.10
3⇔*	$8.7 \cdot 10^9$		
3⇔18	$1.8 \cdot 10^9$	6	2.50
8/11⇔18	$2.7 \cdot 10^9$	12	2.63
8/11⇔*	$1.2 \cdot 10^{10}$		
*⇔18	$6.6 \cdot 10^9$		
9/10⇔8/11	$1.9 \cdot 10^9$		
9/10⇔*	$2.5 \cdot 10^9$		
9/10⇔18	$1.2 \cdot 10^8$	6	3.93

* = 4-7, 12-16 overlapped peaks, [#] reference distance

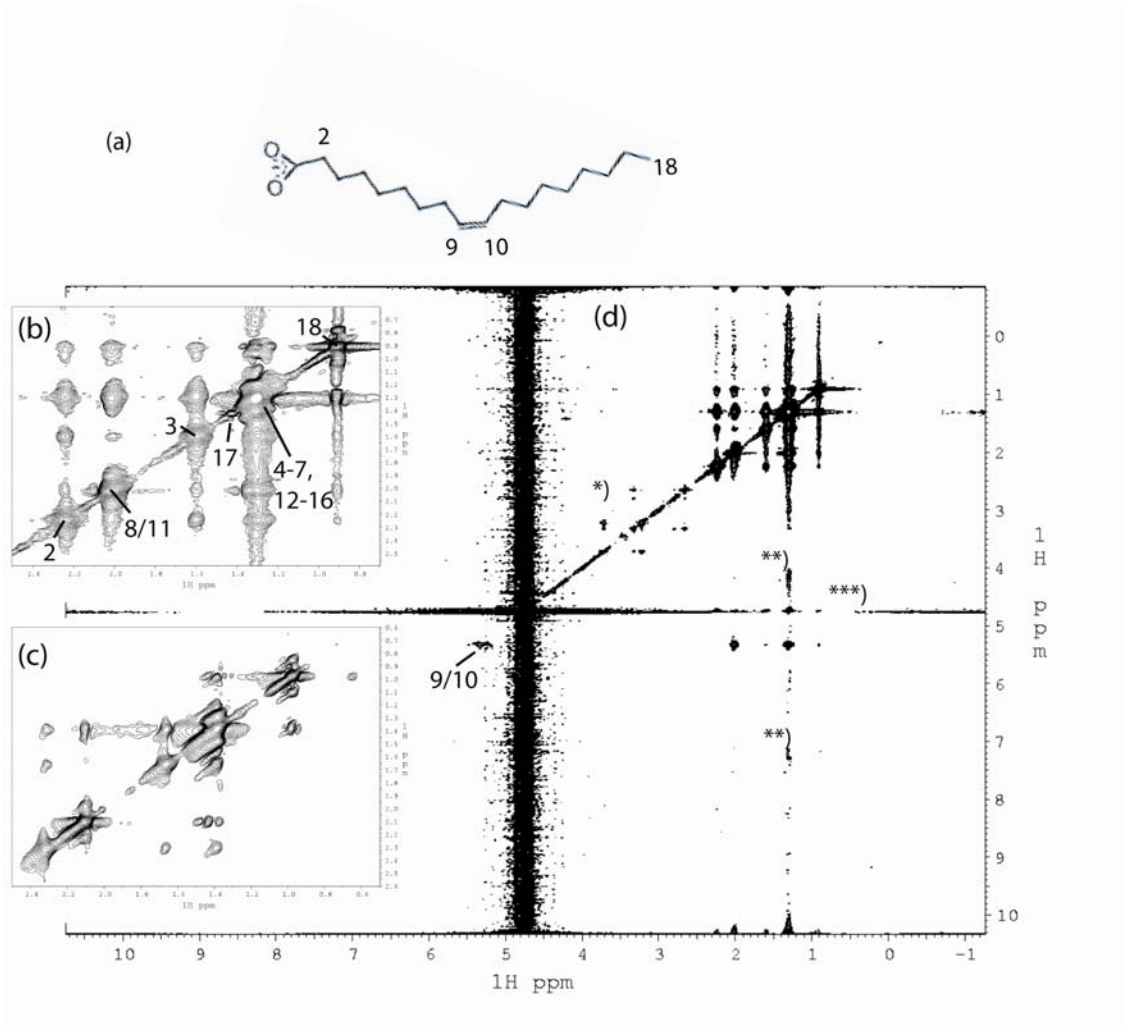

Fig. 1

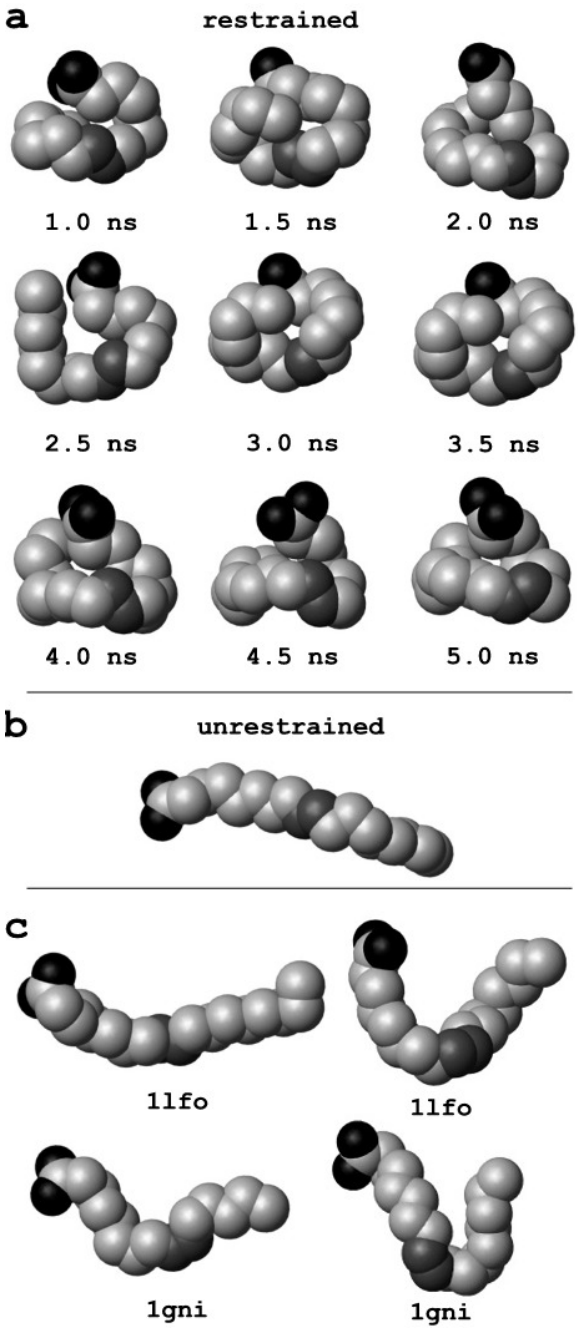
a
restrained
1.0 ns
1.5 ns
2.0 ns
2.5 ns
3.0 ns
3.5 ns
4.0 ns
4.5 ns
5.0 ns
b
unrestrained
c
1lfo
1lfo
1gni
1gni

Fig. 2

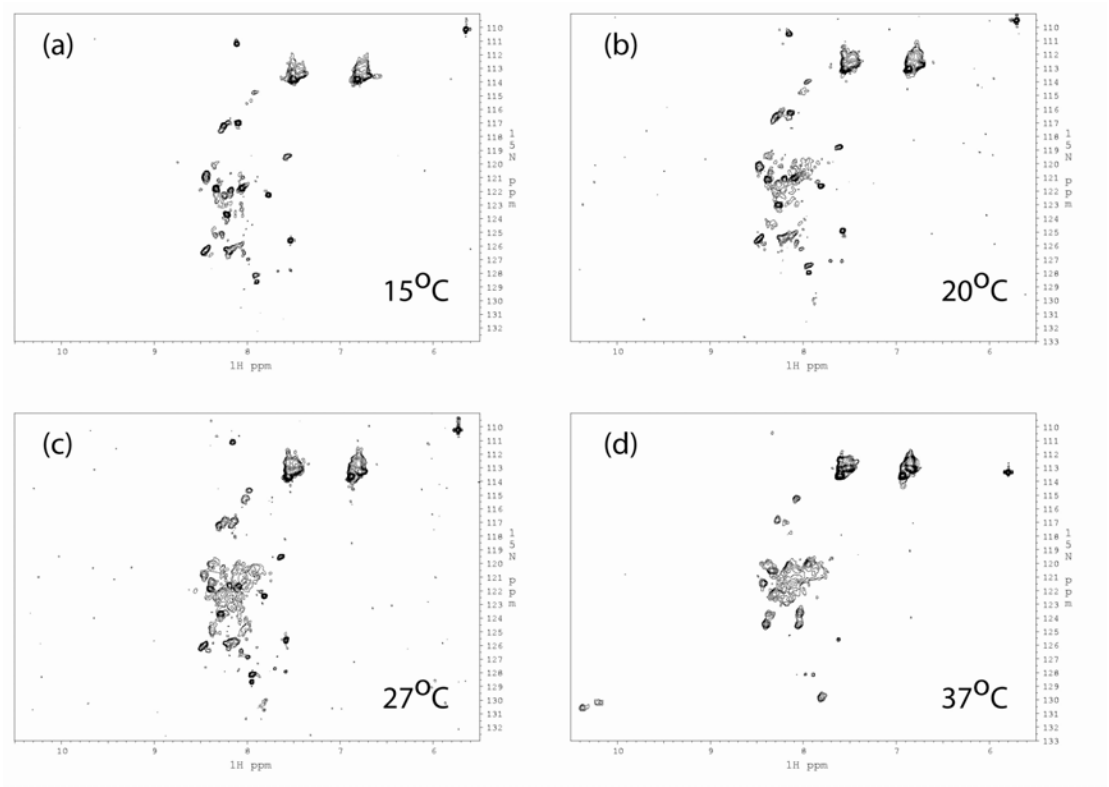

Fig. 3